Electronic Supplementary Information
Interstitial and Substitutional Doping of Mn^{2+} in 2D PEA_2PbBr_4 and BA_2PbBr_4 Perovskites

Udara M. Kuruppu,[a] Alvaro J. Magdaleno,[c,d], Anuraj S. Kshirsagar,[a] Bruno Donnadieu,[a] Ferry Prins*[c,d] and Mahesh K Gangishetty*[a,b]

[a]Department of Chemistry, Mississippi State University, Mississippi State, Mississippi 39762, United States†
[b]Department of Physics and Astronomy, Mississippi State University, Mississippi State, Mississippi 39762, United States†
[c]Condensed Matter Physics Center (IFIMAC), Autonomous University of Madrid, 28049, Madrid, Spain
[d]Department of Condensed Matter Physics, Autonomous University of Madrid, 28049, Madrid, Spain.
Email: mg2234@msstate.edu and ferry.prins@uam.es

Experimental Methods

Chemicals

Lead bromide ($PbBr_2$, 99.999%), Phenethylammonium bromide ($C_8H_{12}BrN$, 98%), n-Butylammonium bromide ($C_4H_{12}BrN$, 98%), Manganese (II) bromide ($MnBr_2$, 98%), Hydrobromic acid (HBr, 48%), and Nitric acid (HNO_3, ≥99.999% trace metals basis) were purchased from Sigma-Aldrich and used as received.

Material synthesis

Both PEA_2PbBr_4 and BA_2PbBr_4 crystals were synthesized by hydrobromic acid-initiated precipitation method, as described below.

Synthesis of pristine and Mn^{2+} doped PEA_2PbBr_4 crystals

In a 20 mL glass vial, 305 mg $PbBr_2$ (0.833 mmol), and 335 mg $C_8H_{12}BrN$ (1.66 mmol) were dissolved using 10 mL of HBr. Subsequently, a vial containing the reaction mixture was placed in an oil bath and the temperature was raised to 120°C while monitoring the temperature of the oil using a digital thermometer. The reaction mixture was constantly stirred for about 15 minutes until to obtain a clear and transparent solution. Then, the stirring was stopped, and the solution was allowed to cool to room temperature (~25 °C) at a controlled cooling rate of 0.5°C/min. Finally, all the crystals were suction-filtered and dried under reduced pressure. For the synthesis of Mn^{2+} doped PEA_2PbBr_4, the process is the same as described above only difference is the addition of various amounts of $MnBr_2$ (to maintain Mn^{2+}: Pb^{2+}precursor mole ratios of 1:0.2, 1:0.5, 1:1, and 4:1) along with other precursors.

Synthesis pristine and Mn^{2+} doped BA_2PbBr_4 crystals

The procedure is the same as described above only difference is the addition of 256 mg (1.66 mmol) of $C_4H_{12}BrN$ and various amounts of $MnBr_2$ (to maintain Pb^{2+}: Mn^{2+}precursor mole ratios of 1:0.5, 1:1, and 4:1) along with other precursors.

ICP-MS elemental analysis

Exactly 10.0 mg of each crystal flake were acidified with conc. HNO_3(70%, ≥99.999% trace metals basis). Subsequently, the reaction mixture was immersed in an oil bath and heated to 100°C until it reached a boil. Upon reaching this temperature, the reaction mixture became clear and transparent, exhibiting no further changes in its appearance. After cooling to room temperature (approximately 25°C), the reaction mixture was transferred to a 100 mL volumetric flask and diluted to the mark with ASTM-type 1 ultrapure water. Finally, the ICP-MS analysis (Perkin Elmer ELAN DRC II ICP-MS) was conducted, and Mn2+ concentrations were calculated for each sample using a calibration curve considering the limits of detection (LOD) from matrix-matched calibration blanks and standards.[1]

Structural characterization

The single-crystal X-ray diffraction (scXRD) of the crystals is measured at 100K, using a three circles goniometer geometry with a fixed Chi angle at 54.74° Bruker AXS D8 Venture, equipped with a Photon III Mixed Mode X-ray detection. A monochromatized Mo X-ray radiation (λ = 0.71073 Å) was selected for the measurement. All frames were integrated with the aid of the Bruker SAINT software[2] using a narrow-frame algorithm. Data were corrected for absorption effects using the multi-scan method (SADABS).[3] Crystals are solved and refined using Bruker SHELXT Software Package.[4] Refinement of the structure was carried out by least squares procedures on weighted F2 values using the SHELXTL-2019/1 included in the APEX5 v2023, 9.4, AXS Bruker program.[5] On the basis of the final model, the density was calculated using Mercury V.4.2.0: (https://www.ccdc.cam.ac.uk/) and POV-Ray v 3.7: (The Persistence of Vision Ray tracer, high quality, Free Software tool) softwares. The crystal structure visualization, and interpretation was done using VESTA software.[6] The Powder X-ray Diffraction (pXRD) is recorded using PROTO, AXRD benchtop powder diffraction system equipped with Cu Kα (1.54 Å) radiation.

Optical and photophysical measurements

Diffuse reflectance spectra (as crystals have internal inhomogeneities) are recorded using Shimadzu UV-2600i UV-Visible spectrophotometer. The Kubelka-Munk (K-M) model is used to transform the diffuse reflectance spectra into absorbance spectra.[7] The band gap for pristine perovskites was obtained using Tauc plot.[8] The steady-state photoluminescence (PL) and photoluminescence excitation (PLE) spectra were recorded using Edinburgh FS5 spectrofluorometer. Photoluminescence quantum yield (PLQY) of all the samples were measured using an integrating sphere calibrated against a Newport photodetector; by following the method described by Mello et al.[9] A 365 nm LED (Thorlabs) excitation source was used as the excitation

source for the PLQY measurements. Time-resolved photoluminescence (TRPL) measurements were recorded with a Deltaflex modular fluorescence lifetime system from Horiba Scientific. A 356 nm LED excitation source was used as the excitation source for the TRPL measurements.

Transient Photoluminescence Microscopy (TPLM) was performed using a home-built scanning avalanche photodiode setup as described in detail by Seitz et al . TPLM was performed on single crystalline flakes of approximately 100 nm thickness using a 405 nm pulsed laser source at 40 MHz repetition rate and a fluence of 50 nJ cm−2 at near-diffraction limited excitation using a ×100 oil immersion objective (Nikon CFI Plan Fluor, NA = 1.3).

Table S1. Single crystal XRD refinement results for PEA_2PbBr_4.

Compound	PEA_2PbBr_4
Chemical formula	$C_{32}H_{48}Br_8N_4Pb_2$
Formula weight/ $gmol^{-1}$	1542.40
Temperature/ K	100
Wavelength/ Å	0.71073
Crystal size/ mm^3	0.325 x 0.491 x 0.504
Crystal system	triclinic
Space group	P -1
a / Å	11.5284(7)
b/ Å	11.5361(7)
c/ Å	17.3101(11)
α/ °	73.977(3)
β/ °	80.337(3)
γ/ °	89.930(3)
Volume/ $Å^3$	2178.8(2)
Z	2
Density (calculated)/ g/cm^3	2.351
Absorption coefficient/ mm^{-1}	15.079
F (000)	1424
Theta range for data collection/ °	1.84 to 30.51
Index ranges	-16<=h<=16, -16<=k<=16, -24<=l<=24
Reflections collected	155888
Independent reflections	13206 [R(int) = 0.1087]
Coverage of independent reflections/ %	99.2
Max. and min. transmission	0.0840 and 0.0490
Refinement method	Full-matrix least-squares on F^2
Refinement program	SHELXL-2019/1 (Sheldrick, 2019)
Function minimized	$\Sigma w (F_o^2 - F_c^2)^2$
Data / restraints / parameters	13206 / 0 / 420
Goodness-of-fit on F^2	1.103
Final R indices, 4423 data; I>2σ(I)	R1 = 0.0679, wR2 = 0.1890
Final R indices all data	R1 = 0.0910, wR2 = 0.2131
Weighting scheme	$w=1/[\sigma^2(F_o^2) +(0.1407P)^2+9.5869P]$ where $P=(F_o^2+2F_c^2)/3$
Largest diff. peak and hole/ $eÅ^{-3}$	4.707 and -4.833
R.M.S. deviation from mean/ $eÅ^{-3}$	0.707

Table S2. Single crystal XRD refinement results for BA_2PbBr_4.

Compound	BA_2PbBr_4
Chemical formula	$C_4H_{12}Br_2NPb_{0.50}$
Formula weight/ $gmol^{-1}$	337.56
Temperature/ K	100
Wavelength/ Å	0.71073
Crystal size/ mm^3	0.202 x 0.346 x 0.479
Crystal system	orthorhombic
Space group	P b c a
a / Å	8.2490(8)
b/ Å	8.1326(8)
c/ Å	27.428(3)
α/ °	90
β/ °	90
γ/ °	90
Volume/ $Å^3$	1840.0(3)
Z	8
Density (calculated)/ g/cm^3	2.437
Absorption coefficient/ mm^{-1}	17.836
F (000)	1232
Theta range for data collection/ °	2.88 to 30.50
Index ranges	-10<=h<=11, -11<=k<=10, -37<=l<=37
Reflections collected	53118
Independent reflections	2636 [R(int) = 0.0736]
Coverage of independent reflections/ %	93.9
Max. and min. transmission	0.1230 and 0.0430
Refinement method	Full-matrix least-squares on F^2
Refinement program	SHELXL-2019/1 (Sheldrick, 2019)
Function minimized	$\Sigma w (F_o^2 - F_c^2)^2$
Data / restraints / parameters	2636 / 0 / 72
Goodness-of-fit on F^2	1.201
Final R indices, 4423 data; I>2σ(I)	R1 = 0.0758, wR2 = 0.2315
Final R indices all data	R1 = 0.0877, wR2 = 0.2503
Weighting scheme	$w=1/[\sigma^2(F_o^2) +(0.1694P)^2+9.4638P]$ where $P=(F_o^2+2F_c^2)/3$
Largest diff. peak and hole/ $eÅ^{-3}$	6.148 and -5.973
R.M.S. deviation from mean/ $eÅ^{-3}$	0.969

Table S3. Elemental analysis of Mn^{2+} doped PEA_2PbBr_4 and BA_2PbBr_4 crystals.

Mn % in Precursor (mole %)	Pb / µM	Mn / µM	Total	Actual Mn doping %	Actual Mn doping % (Round off)
BA Undoped	17.253861	0	17.253861	0	0.00
BA 50% Mn	17.13320463	0.036585366	17.16979	0.213079868	0.21
BA 100% Mn	12.78957529	0.09119039	12.88076568	0.707957833	0.71
BA 400% Mn	15.2027027	0.31488897	15.51759167	2.029238663	2.03
PEA Undoped	18.27944015	0	18.27944015	0	0.00
PEA 50% Mn	15.92664093	0.122679286	16.04932021	0.7643893	0.76
PEA 100% Mn	13.93581081	0.353112486	14.2889233	2.47123229	2.47
PEA 400% Mn	19.48600386	0.997451766	20.48345563	4.869548302	4.87

Table S4. Time-resolved photoluminescence analysis (TRPL) of PEA_2PbBr_4.

The tables below present best-fit parameter values obtained for the photoluminescence (PL) decay of pristine and Mn^{2+} doped PEA_2PbBr_4. The PL decay plots were fitted to a tri-exponential decay function, and the average lifetime (τ_{avg}) was calculated using the equation, $\tau_{avg} = (A_1\tau_1^{\,2} + A_2\tau_2^{\,2} + A_3\tau_3^{\,2})/ (A_1\tau_1 + A_2\tau_2 + A_3\tau_3)$. Where τ_1, τ_2, and τ_3 are lifetimes of tri-exponential decays with relative amplitude percentages A_1, A_2, and A_3 respectively.

Sample (TRPL @ 430 nm)	A_1 (%)	τ_1 (ns)	A_2 (%)	τ_2 (ns)	A_3 (%)	τ_3 (ns)	τ_{avg} (ns)
Prestine	20.9	3.83	64.25	10.14	14.82	36.04	8.19
0.7% Mn doped	51.57	3.04	60.31	7.11	17.82	0.69	2.13
2.4% Mn doped	33.46	0.64	63.05	1.51	3.51	6.98	1.06
4.8% Mn doped	53.09	2.75	7.98	11.12	38.93	0.32	0.78

Sample (TRPL @ 600 nm)	A_1 (%)	τ_1 (µs)	A_2 (%)	τ_2 (µs)	A_3 (%)	τ_3 (µs)	τ_{avg} (µs)
Prestine	-	-	-	-	-	-	-
0.7% Mn doped	18.79	0.99	78.66	4.92	2.54	0.11	1.70
2.4% Mn doped	12.16	0.55	84.32	3.99	3.52	0.67	1.76
4.8% Mn doped	12.88	6.42	84.11	4.19	3.02	0.11	3.12

Table S5. Time-resolved photoluminescence analysis (TRPL) of BA_2PbBr_4.

The tables below present best-fit parameter values obtained for the photoluminescence (PL) decay of pristine and Mn^{2+} doped BA_2PbBr_4.The PL decay plots were fitted to a tri-exponential decay function, and the average lifetime (τ_{avg}) was calculated using the equation, $\tau_{avg} = (A_1\tau_1^{\ 2} + A_2\tau_2^{\ 2} + A_3\tau_3^{\ 2})/ (A_1\tau_1 + A_2\tau_2 + A_3\tau_3)$. Where τ_1, τ_2, and τ_3 are lifetimes of tri-exponential decays with relative amplitude percentages A_1, A_2, and A_3 respectively.

Sample (TRPL @ 435 nm)	A_1 (%)	τ_1 (ns)	A_2 (%)	τ_2 (ns)	A_3 (%)	τ_3 (ns)	τ_{avg} (ns)
Prestine	55.69	3.93	17.97	1.06	26.34	10.56	**2.983**
0.2% Mn doped	15.70	.90	62.91	3.15	21.39	9.11	**2.52**
0.7% Mn doped	12.21	0.63	61.66	3.15	26.13	9.20	**2.40**
2.0% Mn doped	35.94	1.59	24.38	4.67	39.68	0.21	**0.45**

Sample (TRPL @ 600 nm)	A_1 (%)	τ_1 (µs)	A_2 (%)	τ_2 (µs)	A_3 (%)	τ_3 (µs)	τ_{avg} (µs)
Prestine	-	-	-	-	-	-	-
0.2% Mn doped	12.97	7.69	56.12	4.63	30.91	0.39	**1.21**
0.7% Mn doped	16.00	7.47	76.33	4.52	7.68	0.40	**4.38**
2.0% Mn doped	20.05	9.90	75.78	5.78	4.17	3.48	**6.53**

Figure S1. Powder XRD analysis of PEA_2PbBr_4.

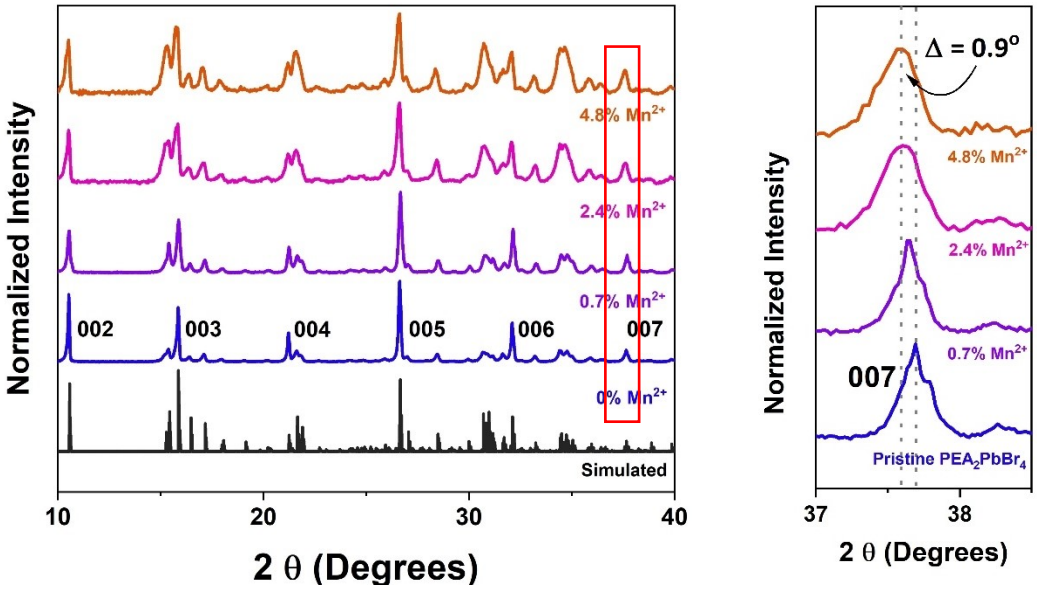

Figure S2. Williamson-Hall plots for microstrain calculations of the PEA_2PbBr_4 (left) and BA_2PbBr_4 (right).

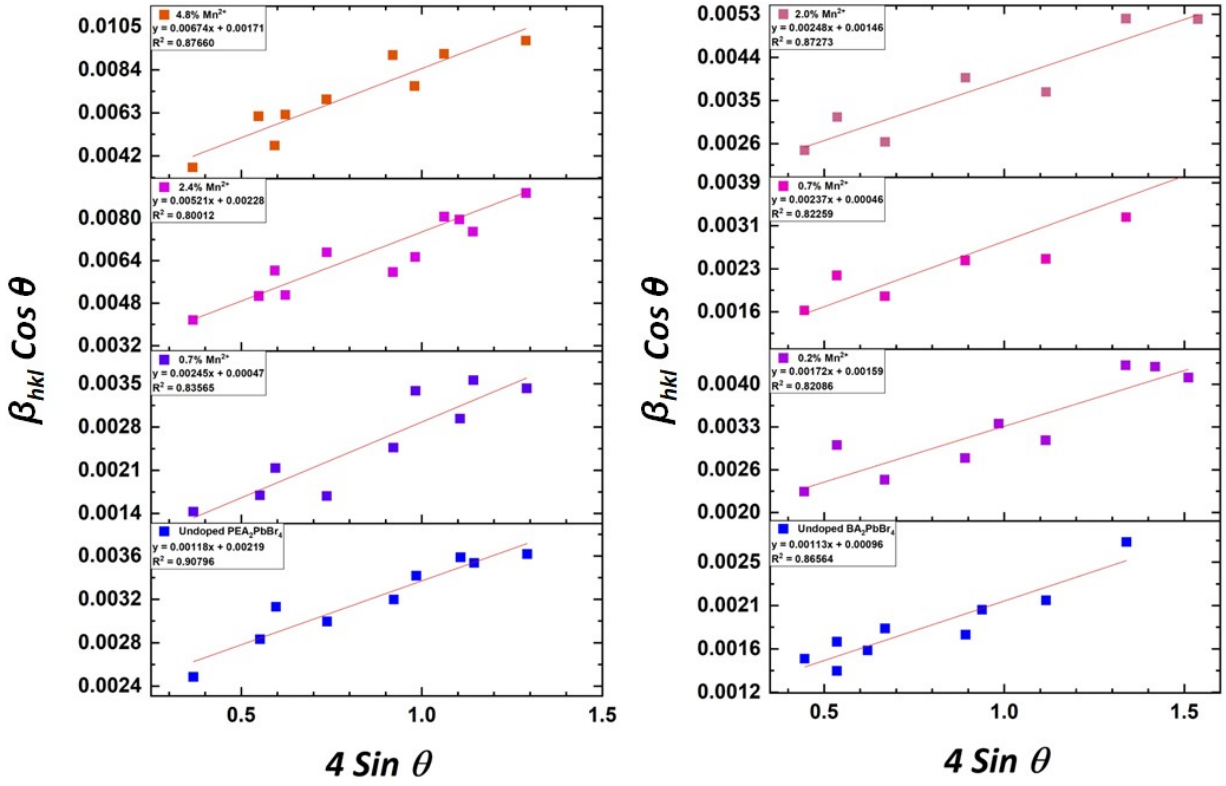

Note: For all calculations, the Uniform Deformation Model (UDM) of the Williamson-Hall method was employed, assuming uniform strain in all crystallographic directions. This model considers the isotropic nature of the 2D perovskite crystal, where all material properties are independent of the in-plane or out-of-plane measurement directions.

Table S6. Calculated microstrain for PEA_2PbBr_4 and BA_2PbBr_4.

Sample	**Average Microstrain**
Undoped BA_2PbBr_4	1.13
0.2% Mn^{2+}: BA_2PbBr_4	1.72
0.7% Mn^{2+}: BA_2PbBr_4	2.37
2.0% Mn^{2+}: BA_2PbBr_4	2.48
Undoped PEA_2PbBr_4	1.18
0.7% Mn^{2+}: PEA_2PbBr_4	2.45
2.4% Mn^{2+}: PEA_2PbBr_4	5.21
4.8% Mn^{2+}: PEA_2PbBr_4	6.74

Figure S3. UV-Vis absorption comparison for PEA_2PbBr_4 and BA_2PbBr_4.

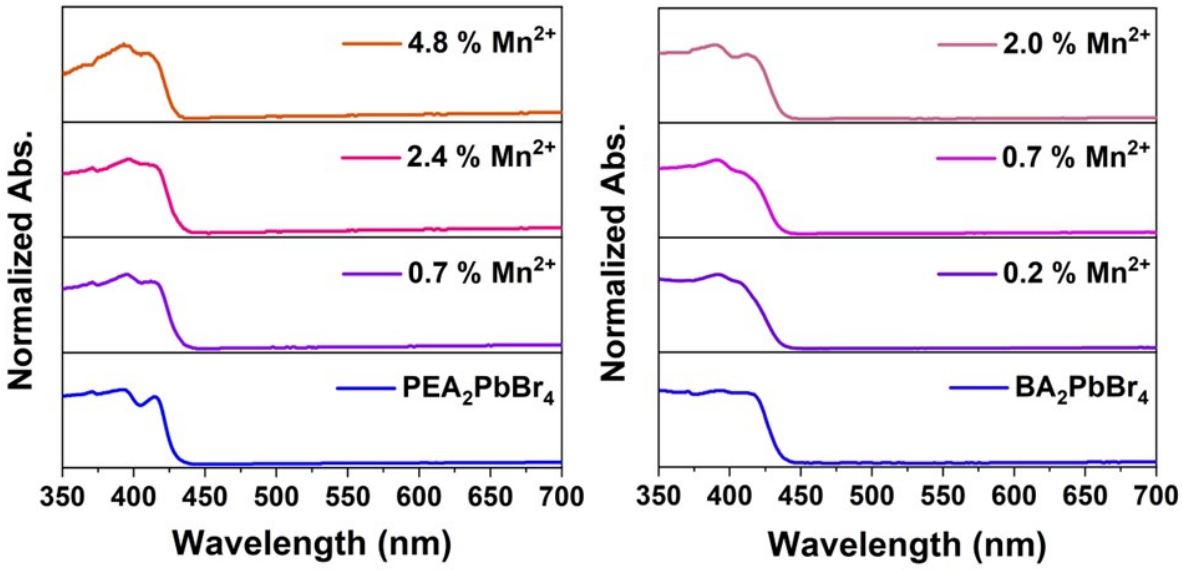

Figure S4. Band-edge calculations for PEA_2PbBr_4 and BA_2PbBr_4.

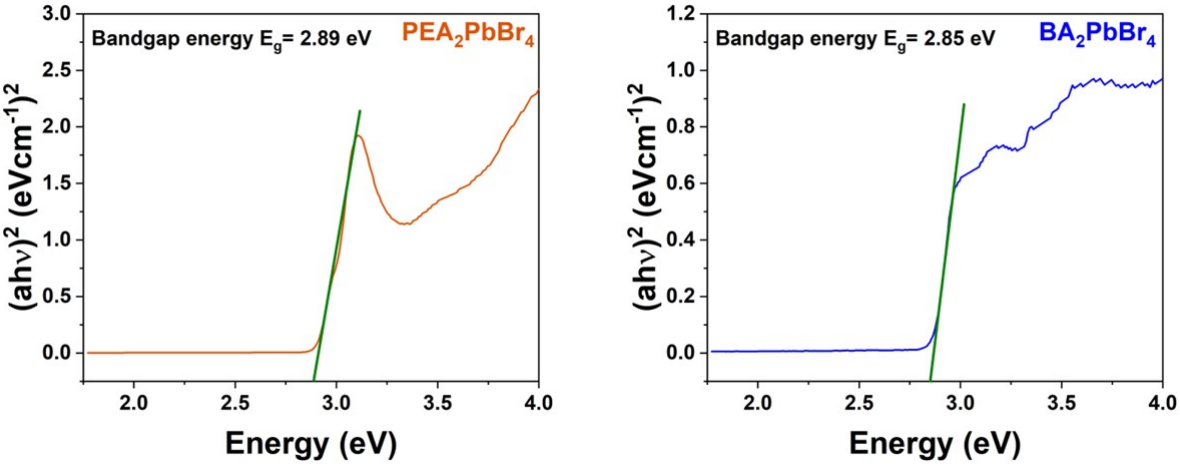

Figure S5. Proposed mechanism for the exciton energy transfer process.

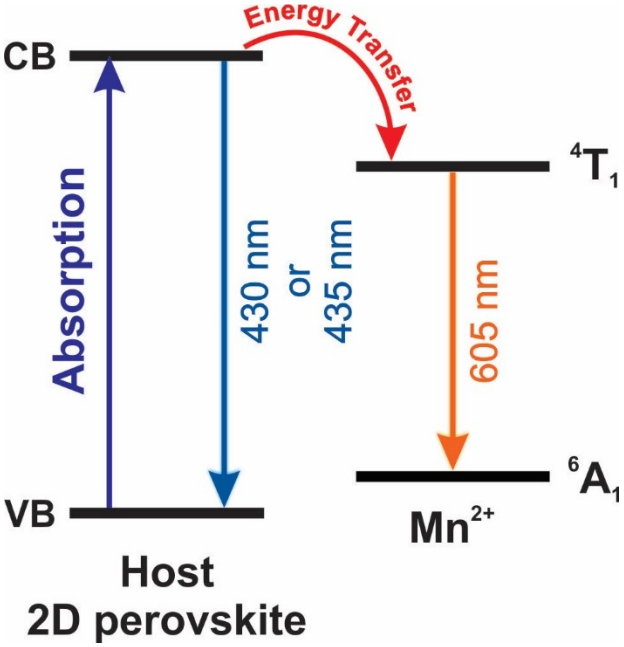

Under the 365 nm excitation, the excitons are formed when electrons in the 2D host perovskite transition from the valence band (VB) to the conduction band (CB). These excitons are then transferred to the $^4T_1$ excited states of Mn^{2+} and subsequently decay to the $^6A_1$ ground state, accompanied by orange emission centered at 600 nm.

Figure S6. PLE spectra of PEA_2PbBr_4 and BA_2PbBr_4.

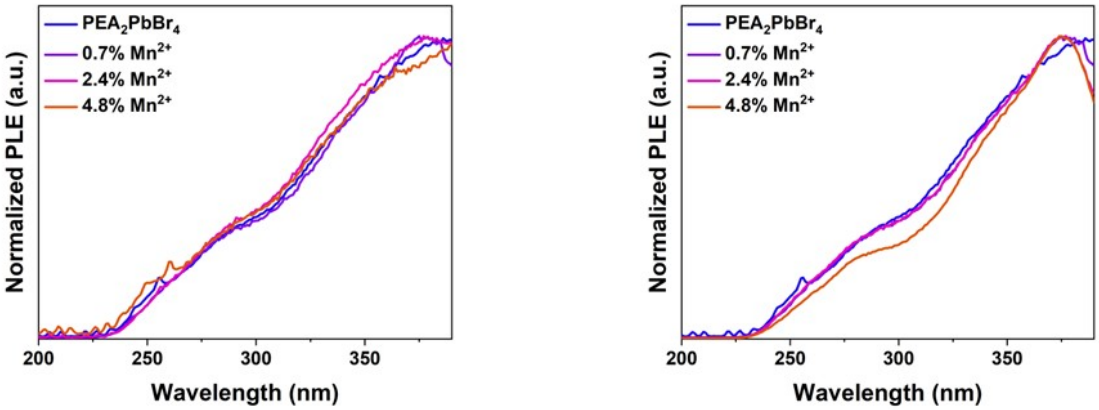

PLE spectra of PEA_2PbBr_4 recorded at 430 nm (left) and at 600 nm (right).

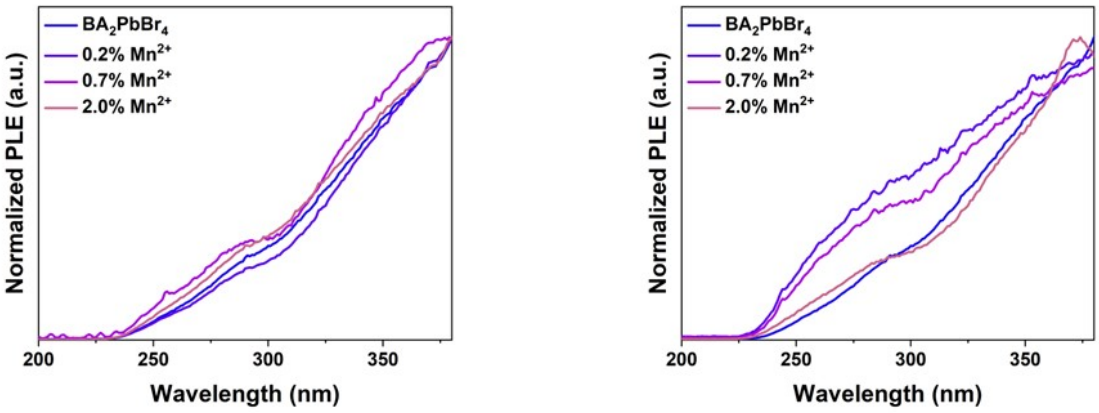

PLE spectra of BA_2PbBr_4 recorded at 435 nm (left) and at 600 nm (right).

Figure S7. PL intensity ratio between dopant and host emission for PEA_2PbBr_4 (top) and BA_2PbBr_4 (bottom).

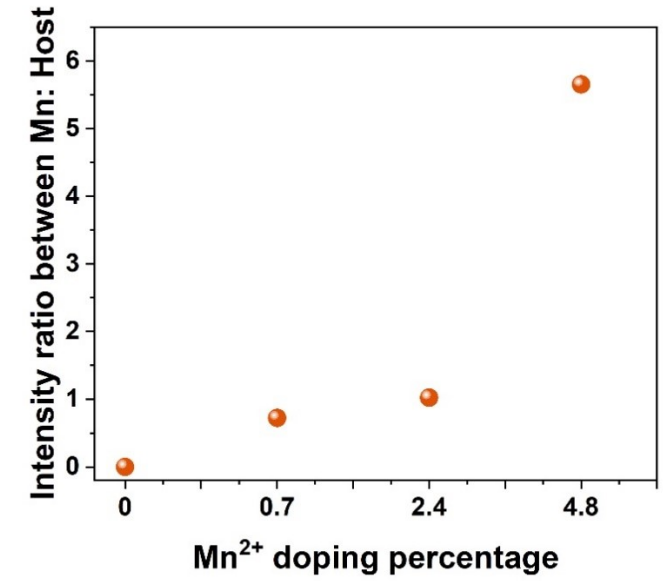

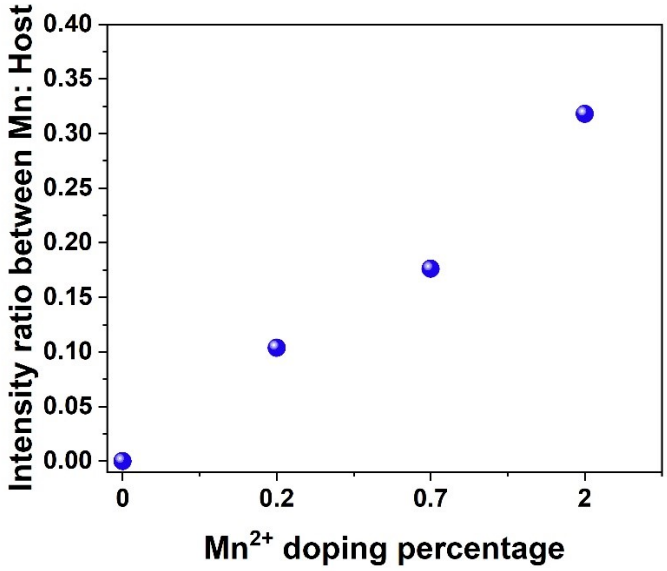

Figure S8. TRPL of PEA_2PbBr_4 and BA_2PbBr_4 recorded at 600 nm.

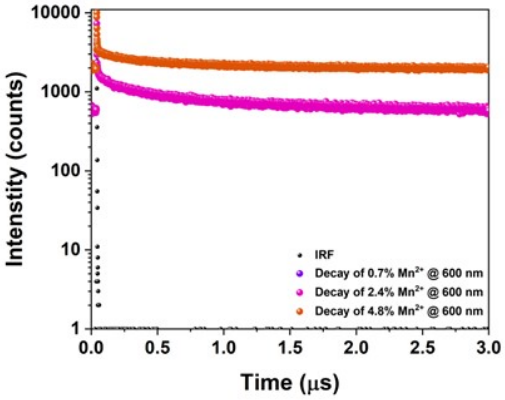

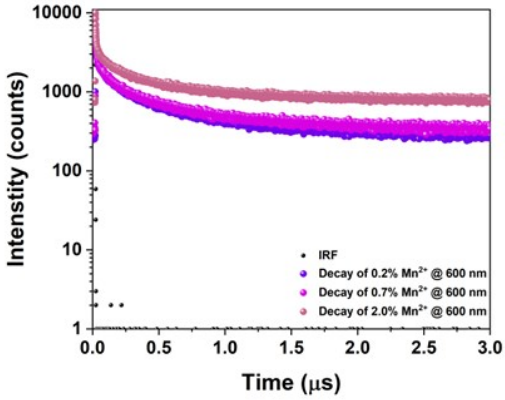

Figure S9. Image of the PEA_2PbBr_4 and BA_2PbBr_4 flakes under 365 nm UV lamp.

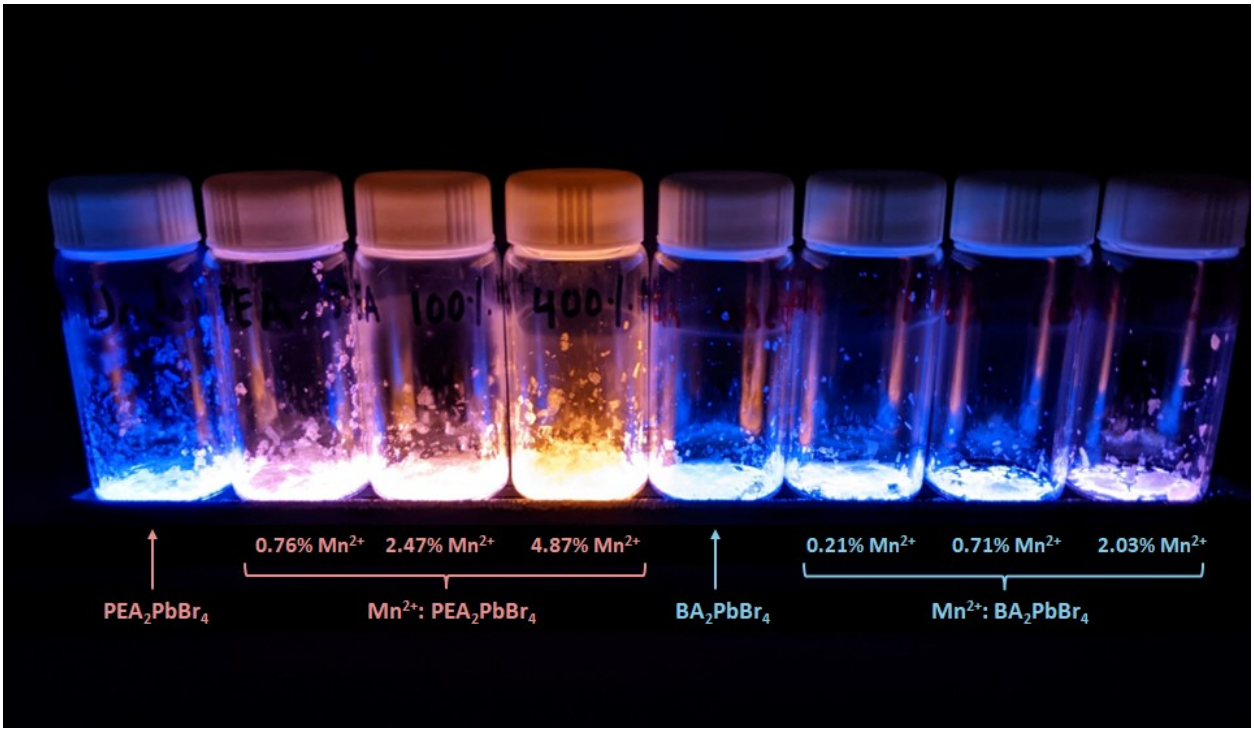

Figure S10. Fluorescence microscopy images of the PEA_2PbBr_4 flakes under 365 nm excitation.

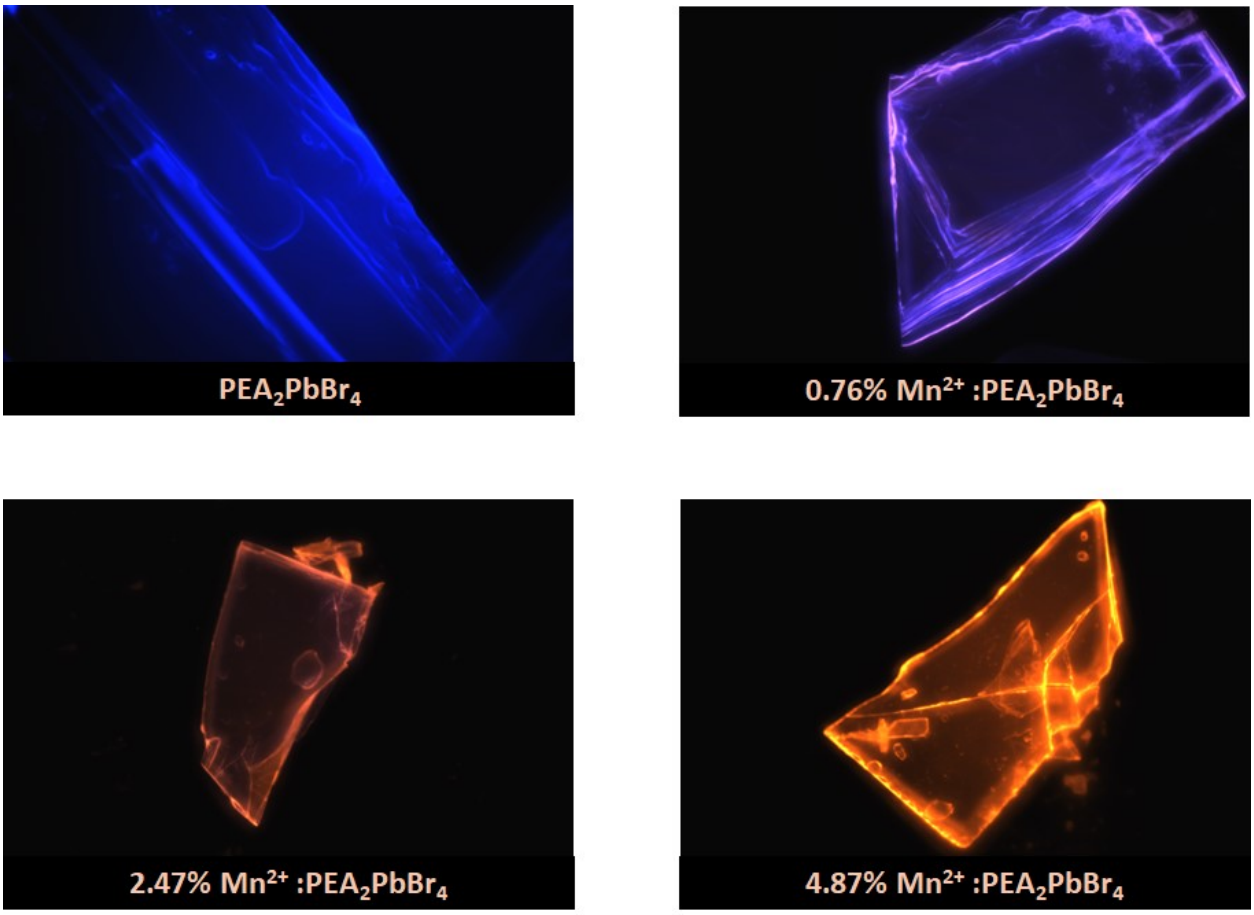

Figure S11. Fluorescence microscopy images of the BA_2PbBr_4 flakes under 365 nm excitation.

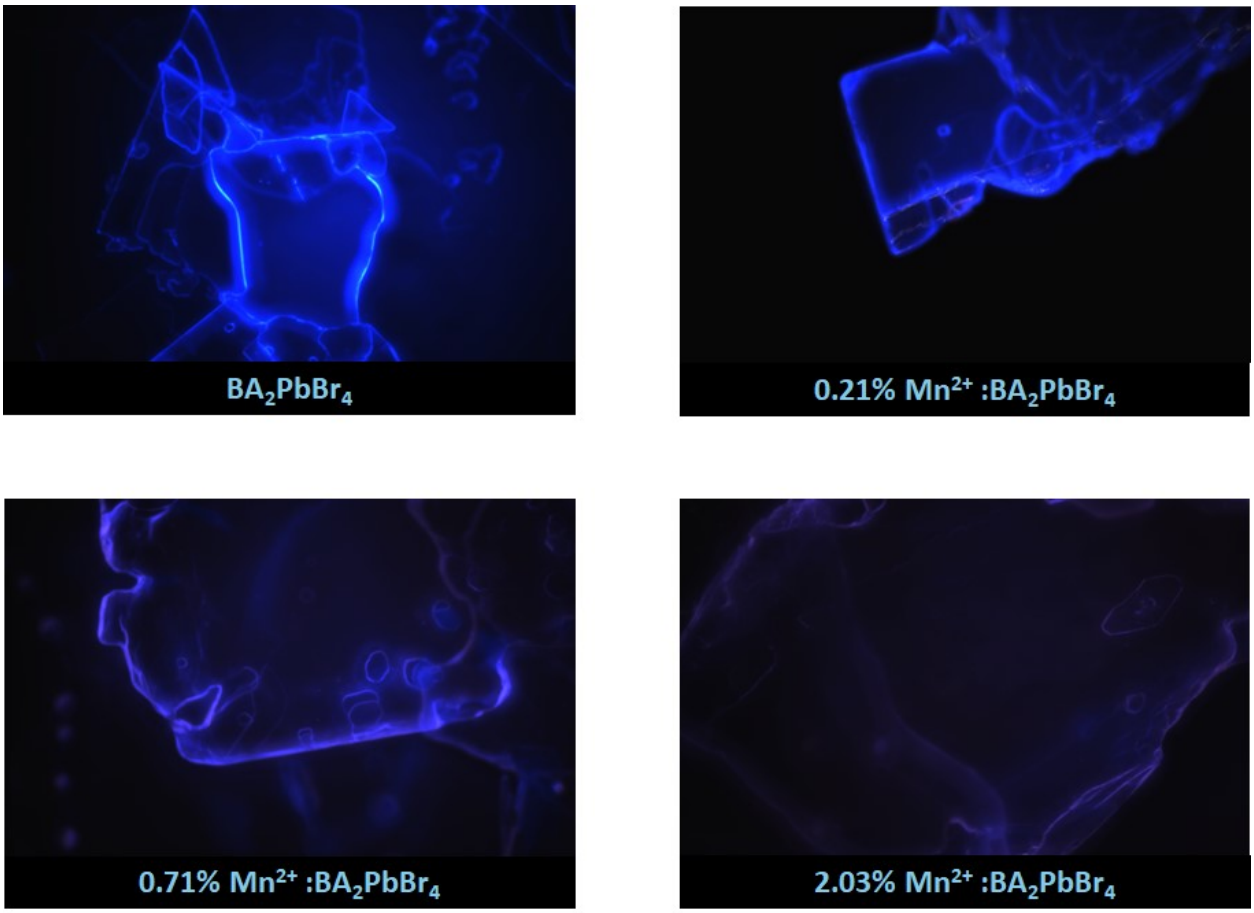

Figure S12. TRPL and PLQY comparison of the PEA_2PbBr_4 (top) and BA_2PbBr_4 (bottom).

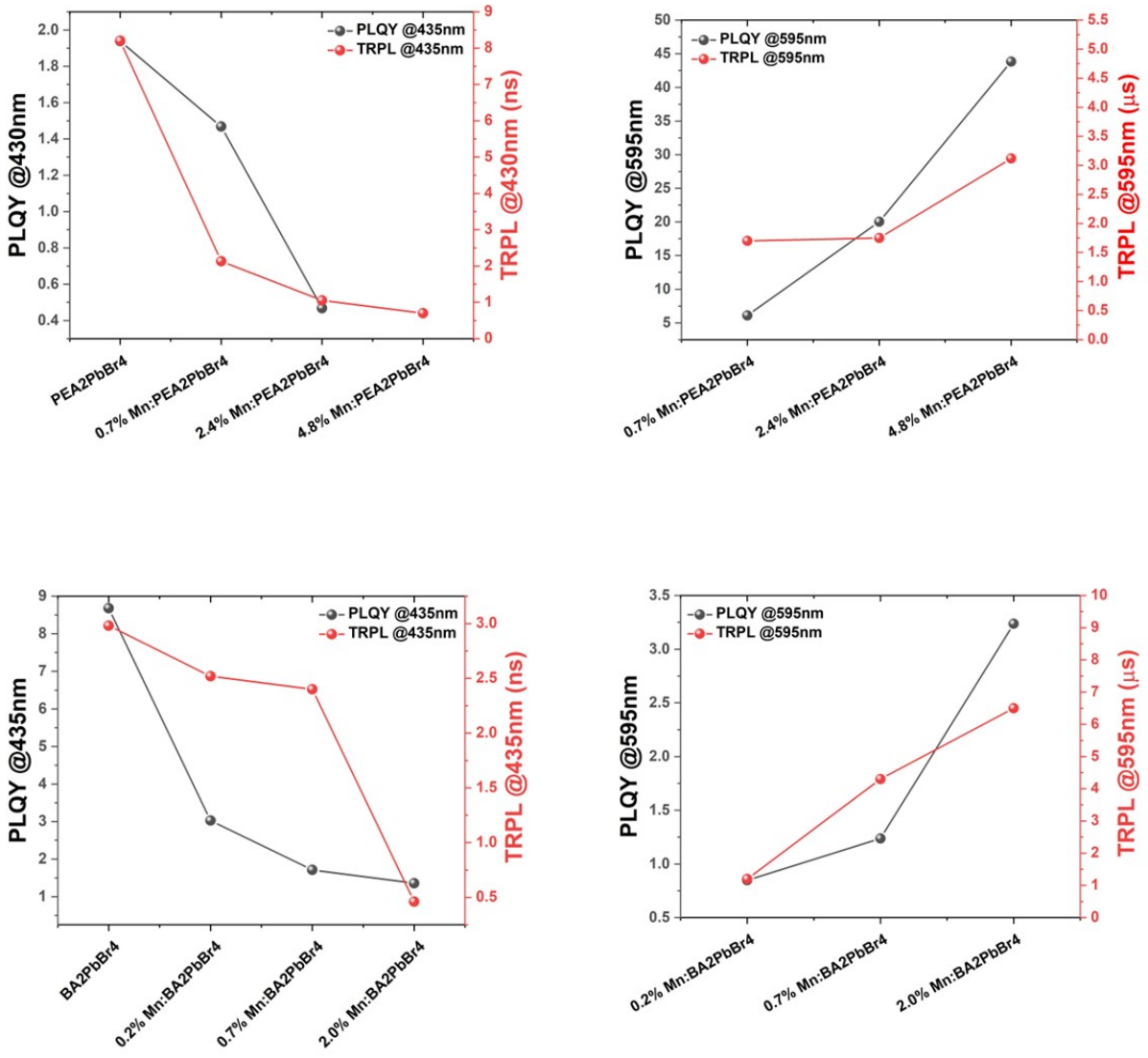

***Note:** The PLQY measured at 595 nm corresponds to the PLQY of Mn2+ emission. It is designated as $PLQY_{Mn}$ in the main text.

Figure S13. PEA_2PbBr_4 and BA_2PbBr_4 crystals with approximately similar Mn^{2+} doping percentages (top) and the PL spectra for the comparison (bottom).

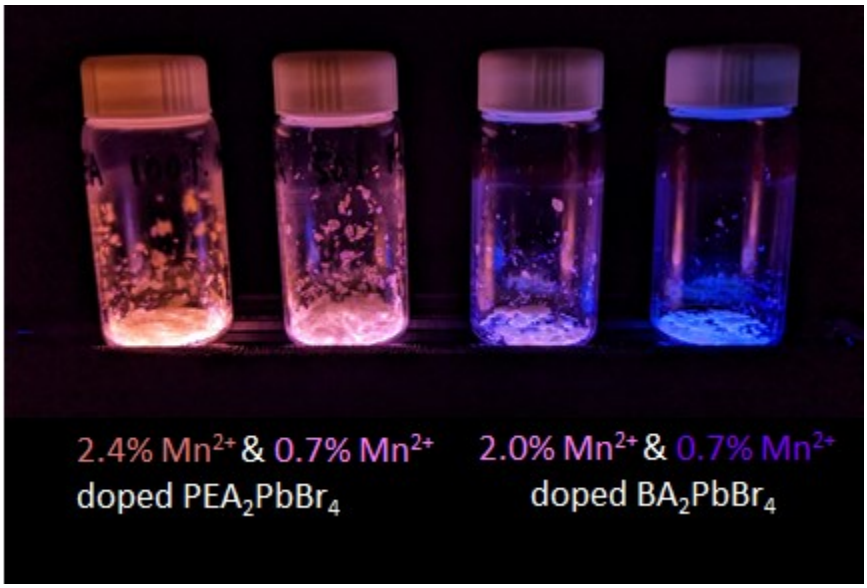

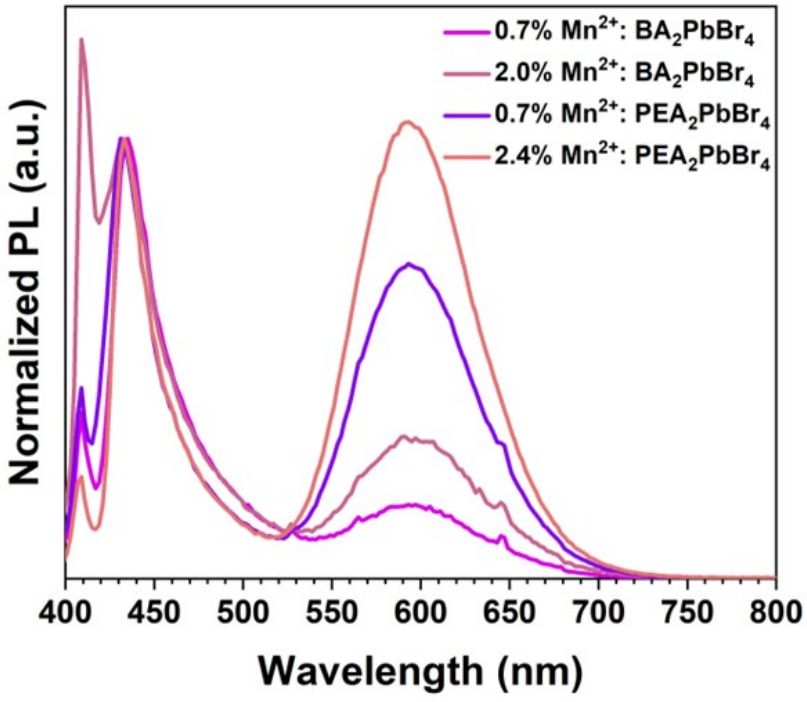

Figure S14. CIE diagrams of PEA_2PbBr_4 (top) and BA_2PbBr_4 (bottom).

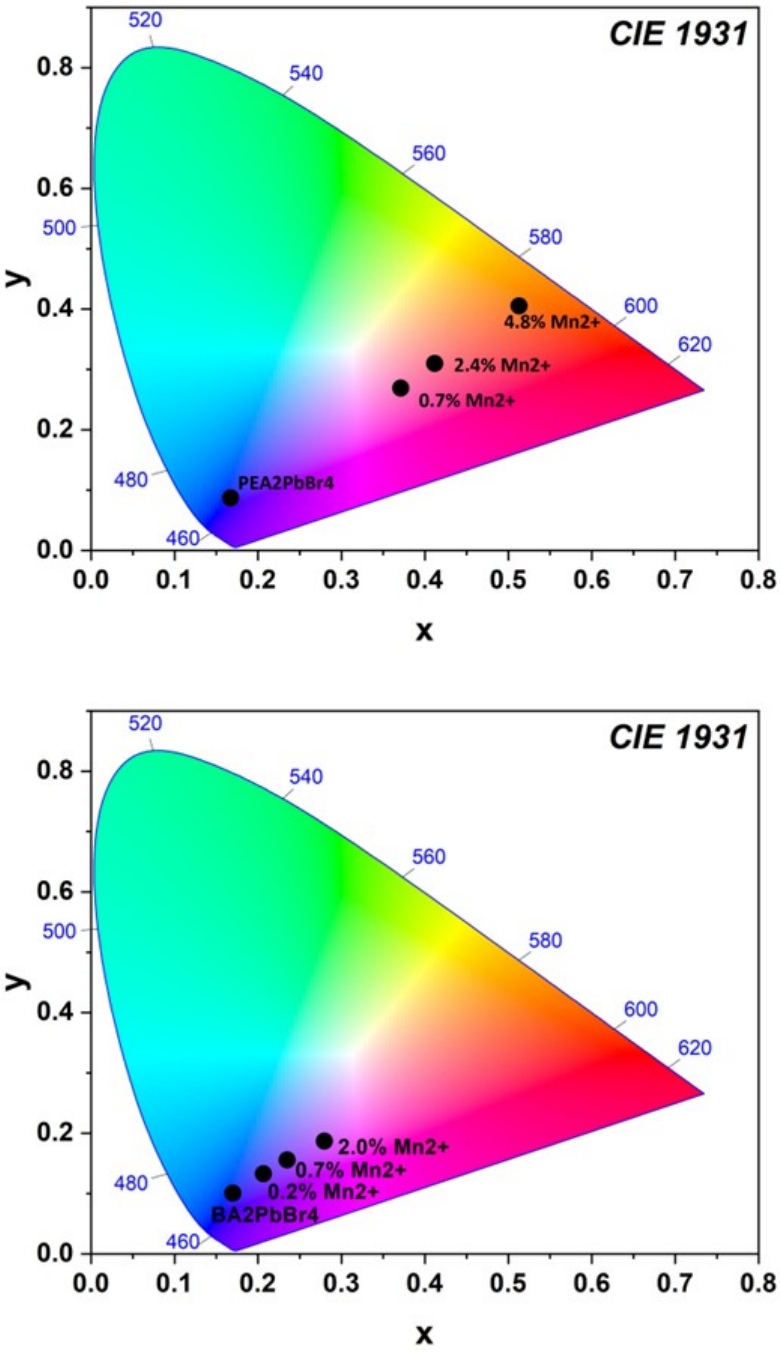

Figure S15. SEM/EDAX analysis for Mn^{2+}: PEA_2PbBr_4.

Spectrum processing: PEA_2PbBr_4

No peaks omitted

Processing option : All elements analyzed (Normalised)

Number of iterations = 3

Standard :

C CaCO3 1-Jun-1999 12:00 AM

N Not defined 1-Jun-1999 12:00 AM

Mn Mn 1-Jun-1999 12:00 AM

Br KBr 1-Jun-1999 12:00 AM

Pb PbF2 1-Jun-1999 12:00 AM

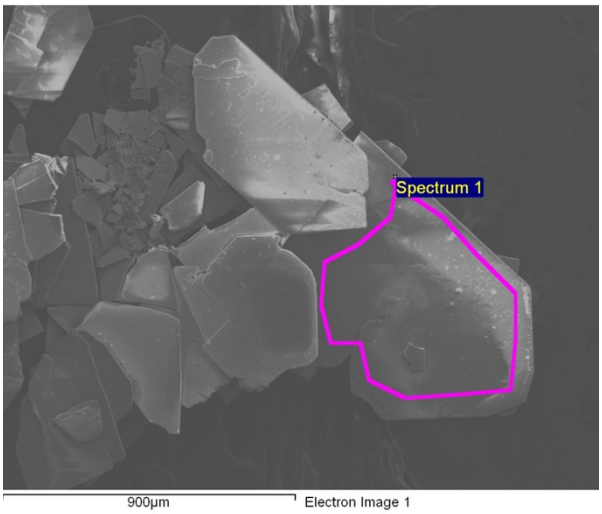

Element	Weight%	Atomic%
C K	32.43	73.06
N K	5.17	9.98
Mn K	1.00	0.49
Br L	40.62	13.75
Pb M	20.78	2.71
Totals	100.00	

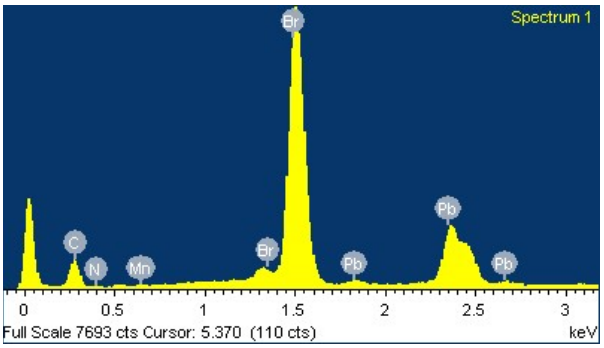

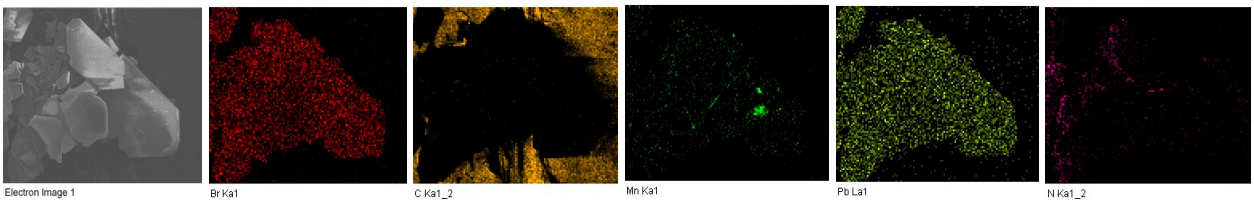

Note: Based on the atomic percentages we obtained from SEM/EDX analysis, approximately 1% of Mn^{2+} is present in PEA_2PbBr_4, while no Mn is detected in BA_2PbBr_4. This is attributed to the lower detection limit of our SEM, which ranges from 0.1 wt% to 1 wt%.[10]

References

1. Deanna R. Jones, Jeffery M. Jarrett, Denise S. Tevis, Melanie Franklin, Neva J. Mullinix, Kristen L. Wallon, C. Derrick Quarles, Kathleen L. Caldwell, Robert L. Jones, Talanta, 2017, 162, 114-122
2. Saint Program included in the package software: APEX5 v2023, 9.2.
3. Sadabs, Blessing R.H. (1995), Acta Cryst. A51. 33-38. Blessing, R. H. (1995) An empirical correction for absorption anisotropy. Acta Crystallographica Section A Foundations of Crystallography, 51 (1). 33-38. Multi-Scan (SADABS); Krause and al., 2015).
4. SHELXT-Integrated space-group and crystal-structure determination Sheldrick, G. M. Acta Crystallogr., Sect. A 2015, A71, 3-8.
5. APEX5 v2023, 9.2, AXS Bruker program.
6. Momma, K.; Izumi, F., VESTA 3 for three-dimensional visualization of crystal, volumetric and morphology data. J. Appl. Crystallogr. 2011, 44 (6), 1272-1276.6
7. T. Eickhoff, P. Grosse and W. Theiss, Vib Spectrosc, 1990, 1, 229–233.
8. P. Makuła, M. Pacia and W. Macyk, *Journal of Physical Chemistry Letters*, 2018, **9**, 6814–6817.
9. J. C. De Mello, H. F. Wittmann and R. H. Friend, *Advanced Materials*, 1997, **9**, 230–232.
10. R. R. Samal, D. Gautam, K. Panmei, P. Lanbiliu, L. Saya, G. Gambhir, S. Hooda and S. Kumar, in Comprehensive Materials Processing (Second Edition), ed. S. Hashmi, Elsevier, Oxford, 2024, pp. 210–220.